BIOCHEMISTRY
including biophysical chemistry & molecular biology

Article

pubs.acs.org/biochemistry

Comparisons of Interfacial Phe, Tyr, and Trp Residues as Determinants of Orientation and Dynamics for GWALP Transmembrane Peptides

Kelsey A. Sparks, Nicholas J. Gleason, Renetra Gist, Rebekah Langston, Denise V. Greathouse, and Roger E. Koeppe, II*

Department of Chemistry and Biochemistry, University of Arkansas, Fayetteville, Arkansas 72701, United States

Supporting Information

ABSTRACT: Aromatic amino acids often flank the transmembrane alpha helices of integral membrane proteins. By favoring locations within the membrane–water interface of the lipid bilayer, aromatic residues Trp, Tyr, and sometimes Phe may serve as anchors to help stabilize a transmembrane orientation. In this work, we compare the influence of interfacial Trp, Tyr, or Phe residues upon the properties of tilted helical transmembrane peptides. For such comparisons, it has been critical to start with no more than one interfacial aromatic residue near each end of a transmembrane helix, for example, that of GWALP23 (acetyl-GGALW^{5}(LA)$_{6}$LW^{19}LAGA-[ethanol]amide). To this end, we have employed ^{2}H-labeled alanines and solid-state NMR spectroscopy to investigate the consequences of moving or replacing W5 or W19 in GWALP23 with selected Tyr, Phe, or Trp residues at the same or proximate locations. We find that GWALP23 peptides having F5, Y5, or W5 exhibit essentially the same average tilt and similar dynamics in bilayer membranes of 1,2-dilauroylphosphatidylcholine (DLPC) or 1,2-dioleoylphosphatidylcholine (DOPC). When double Tyr anchors are present, in Y^{4,5}GWALP23 the NMR observables are markedly more subject to dynamic averaging and at the same time are less responsive to the bilayer thickness. Decreased dynamics are nevertheless observed when ring hydrogen bonding is removed, such that F^{4,5}GWALP23 exhibits a similar extent of low dynamic averaging as GWALP23 itself. When F5 is the sole aromatic group in the N-interfacial region, the dynamic averaging is (only) slightly more extensive than with W5, Y5, or Y4 alone or with F4,5, yet it is much less than that observed for Y^{4,5}GWALP23. Interestingly, moving Y5 to Y4 or W19 to W18, while retaining only one hydrogen-bond-capable aromatic ring at each interface, maintains the low level of dynamic averaging but alters the helix azimuthal rotation. The rotation change is about 40° for Y4 regardless of whether the host lipid bilayer is DLPC or DOPC. The rotational change ($\Delta\rho$) is more dramatic and more complex when W19 is moved to W18, as $\Delta\rho$ is about +90° in DLPC but about −60° in DOPC. Possible reasons for this curious lipid-dependent helix rotation could include not only the separation distances between flanking aromatic or hydrophobic residues but also the absolute location of the W19 indole ring. For the more usual cases, when the helix azimuthal rotation shows little dependence on the host bilayer identity, excepting W^{18}GWALP23, the transmembrane helices adapt to different lipids primarily by changing the magnitude of their tilt. We conclude that, in the absence of other functional groups, interfacial aromatic residues determine the preferred orientations and dynamics of membrane-spanning peptides. The results furthermore suggest possibilities for rotational and dynamic control of membrane protein function.

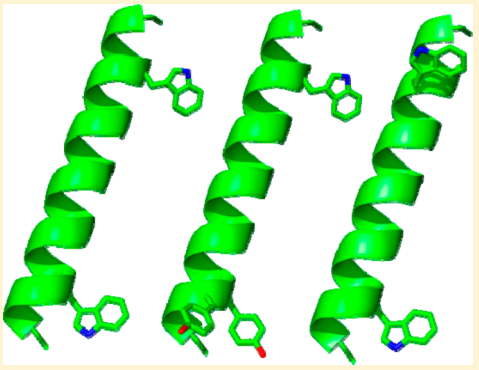

Model peptides have proven to be useful for studying protein–lipid interactions, which in turn are important for the regulation of biological function. Model systems offer particular advantages for establishing general principles because specific changes in peptide sequence and structure can be made, and the direct effects on interaction with a surrounding lipid membrane can be analyzed. Several membrane proteins, including gramicidin channels, reveal the preferred location of tryptophan residues at the lipid–water interface.[1−3] For model peptide design, a core leucine–alanine sequence[4] will enhance sensitivity of the peptide to membrane thickness because of hydrophobic mismatch. Then, by altering the identities or positions of aromatic anchors that flank the core sequence, the effects of these placements on the orientations and dynamics of transmembrane helices can be investigated and inferences for membrane proteins can be deduced.

The early model WALP peptides (acetyl-GWWA-(LA)$_{n}$LWWA-[ethanol]amide), incorporating multiple Trp (W) anchors and the helical, hydrophobic repeating Leu–Ala core sequence, were important for helping to establish principles for the interfacial partitioning of Trp residues and the modulation of lipid phase behavior.[4] Later, the four Trp residues were mutated to other aromatic or charged residues

Received: April 10, 2014
Revised: May 13, 2014
Published: May 14, 2014

   dx.doi.org/10.1021/bi500439x | *Biochemistry* 2014, 53, 3637−3645

(Tyr, Phe, Lys, Arg, or His) to monitor the importance of the chemical and physical properties.[5,6] The WALP family peptides adopt specific preferred tilted transmembrane orientations in lipid bilayer membranes,[7,8] but, in addition to cone precession about the membrane normal,[9] they also experience excessive dynamic averaging of solid-state NMR observables,[10−13] caused by the presence of the four Trp residues.[14] Importantly, the extent of dynamic averaging can be greatly reduced by decreasing the number of aromatic residues, as in GWALP23 (acetyl-GGALW(LA)$_6$LWLAGA-[ethanol]amide),[15] which possesses only two Trp residues and still maintains a preferred and well-defined tilted orientation[12,14,16] with low dynamic averaging. The tryptophans in GWALP23 thereby flank a hydrophobic Leu−Ala core of the same length as that of WALP19.[4,7] With fewer aromatic residues, it becomes easier to assess the roles of each of them. The results to date suggest that four Trp anchors are so dominating, and possibly competing,[17] that they induce significant peptide dynamics, mainly because of rotational "slippage" about the helix axis.[14,16]

The favorable properties of GWALP23 have enabled this peptide to be employed as a highly suitable parent host framework for examining the influence of specific charged guest residues within the core hydrophobic sequence.[18,19] It has furthermore been possible to examine the titration behavior of specific residues and the influence of ionization state upon helix orientation.[20] Within the GWALP23 context, questions arose about the effects of changing the identity, number, and position of the aromatic residues. A peptide having a single Trp → Tyr replacement (Y^{5}GWALP23) exhibits similar transmembrane orientation and dynamics as those of GWALP23,[17] in three different lipids, such that the substitution of Tyr for Trp causes no fundamental change in the lipid−peptide interactions. However, when two Tyr residues are introduced to produce Y^{4,5}GWALP23, the extent of dynamic averaging increases dramatically,[17] reminiscent of the earlier WALP peptides.

With the Trp- and Tyr-containing members of the GWALP23 family as a backdrop, we have examined the influence of phenylalanine by altering the Tyr-containing models so as to have non-hydrogen-bonding Phe residues in F^{5}GW^{19}ALP23 and F^{4,5}GW^{19}ALP23 (acetyl-GGAF^{4}F^5(LA)$_6$LW^{19}LAGA-[ethanol]amide). We furthermore examined whether the dynamic behavior shown by Y^{4,5}GW^{19}ALP23 could be caused by Y4 alone, as opposed to the Y4,5 combination. Placing a Tyr residue at position 4 also provided a way of determining the effects of moving a single aromatic residue one position (100°) around the α helix by comparison with Y^{5}GW^{19}ALP23. A similar radial comparison between aromatic ring positions was made by moving Trp19 to position 18 to give GW^{5,18}ALP23.

MATERIALS AND METHODS

Peptides F^{5}GWALP23, F^{4,5}GWALP23, Y^{4}GWALP23, and W^{18}GWALP23 (Table 1) were synthesized on a model 433A synthesizer from Applied Biosystems by Life Technologies (Foster City, CA) using solid-phase methods, as described previously.[17] Typically, two deuterated alanines of differing isotope abundances were incorporated into each synthesized peptide. Peptides were purified as described[19,21] using an octyl silica column (Zorbax Rx-C8, 9.4 × 250 mm, 5 μm particle size; Agilent Technologies, Santa Clara, CA) and a gradient of 97−100% methanol (with 0.1% trifluoroacetic acid) over 28 min. Final peptide purity (>97%) was confirmed by reversed-phase HPLC, and peptide identity, by mass spectrometry (Figure S1 of the Supporting Information).

Table 1. Sequences of GWALP23-Like Peptides with Aromatic Substitutions[a]

name	sequence
WALP23	a-GWW^{3}LALALALALALALALWWA-e
GWALP23	a-GGALW^{5}LALALALALALALWLAGA-e
Y^{5}GWALP23	a-GGALY^{5}LALALALALALALWLAGA-amide
Y^{4,5}GWALP23	a-GGAY^{4}Y^{5}LALALALALALALWLAGA-amide
F^{5}GWALP23	a-GGALF^{5}LALALALALALALWLAGA-amide
F^{4,5}GWALP23	a-GGAF^{4}F^{5}LALALALALALALWLAGA-amide
Y^{4}GWALP23	a-GGAY^{4}LLALALALALALALWLAGA-amide
W^{18}GWALP23	a-GGALW^{5}LALALALALALAW^{18}LLAGA-amide

[a]Abbreviations: a, acetyl; e, ethanolamide.

Solid-state ^{2}H NMR experiments, using mechanically aligned samples, were performed using methods that have been described previously.[17] Mechanically aligned samples (1:60, peptide/lipid; 45% hydration, w/w) were prepared using DOPC, DMPC, or DLPC lipid from Avanti Polar Lipids (Alabaster, AL) and deuterium-depleted water from Cambridge Isotope Laboratories (Andover, MA). Bilayer alignment within each sample was confirmed using ^{31}P NMR at 50 °C on a Bruker (Billerica, MA) Avance 300 spectrometer. Deuterium NMR spectra were recorded at 50 °C using both $\beta = 0°$ (bilayer normal parallel to magnetic field) and $\beta = 90°$ macroscopic sample orientations on a Bruker Avance 300 spectrometer utilizing a quadrupolar echo pulse sequence[22] with 90 ms recycle delay, 3.2 μs pulse length, and 115 μs echo delay. Between 0.6 and 1.5 million scans were accumulated during each ^{2}H NMR experiment. An exponential weighting function with 100 Hz line broadening was applied prior to Fourier transformation.

Helix orientations were analyzed by means of a semistatic "GALA" method based on three adjustable parameters: the average tilt τ_o of the helix axis, the average azimuthal rotation ρ_o about the helix axis, and a principal order parameter S_{zz}, as described.[7,17] An additional three-parameter modified Gaussian method is available, based on τ_o, ρ_o, a distribution width $\sigma\rho$, and a fixed $\sigma\tau$.[16] We also employed this modified Gaussian method, but $\sigma\tau$ was fixed at either 15° (DLPC) or 9° (DOPC; see Discussion) instead of the previously assumed value of 0° for $\sigma\tau$. For the analysis of helix rotation, we analyzed some pairwise residue separation distances using a recently described procedure.[23] Distances were compared to hydrophobic thicknesses of 20.9 Å for DLPC[24] and 27.2 Å for DOPC,[25] which are based on the location D_C of the Gibbs dividing surface for the hydrocarbon region of the bilayer.[25]

RESULTS

The designed peptides (Table 1 and Figure 1) were successfully synthesized and purified, as confirmed by analytical HPLC and MALDI-TOF mass spectrometry (Figure S1 of the Supporting Information). The repeating Leu−Ala sequence at the core of GWALP peptides favors folding into α-helical secondary structure within the hydrophobic region of the lipid bilayer. Indeed, the CD spectra for the new variants of GWALP23 (Figure 2) show a minimum near 208 nm and a broad shoulder near 222 nm, indicating that the secondary structure is indeed α-helical. The ^{31}P NMR spectra for oriented samples of each peptide−lipid combination furthermore confirmed the presence of oriented lipid bilayers within samples that were aligned with

dx.doi.org/10.1021/bi500439x | Biochemistry 2014, 53, 3637−3645

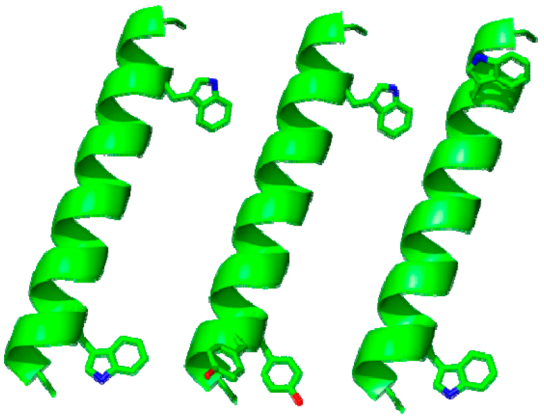

Figure 1. Representative models of GWALP23, $Y^{4,5}$GWALP23, and W^{18}GALP23 (left to right) showing the locations of aromatic side chains on a ribbon helix; drawn using PyMOL.[30] The side-chain orientations are arbitrary.

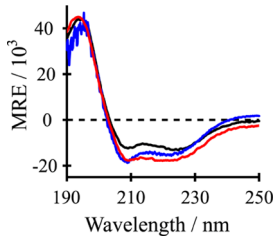

Figure 2. Circular dichroism (CD) spectra of $F^{4,5}$GWALP23 (black), Y^5GWALP23 (blue), and Y^4GWALP23 (red) in DLPC (1:60 peptide/lipid). The *y*-axis units for mean residue ellipticity (MRE) are deg cm^2 $dmol^{-1}$.

the bilayer normal either parallel ($\beta = 0°$) or perpendicular ($\beta = 90°$) to the applied magnetic field. The spectra exhibit characteristic ^{31}P resonances located close to −14.5 ppm for the $\beta = 90°$ orientation and near +29 ppm when $\beta = 0°$ (Figure S2 of the Supporting Information).

Solid-state ^2H NMR spectra from oriented samples of peptide and lipid enable the relative orientations and dynamic behavior of the folded peptide helices to be determined in lipid bilayer membranes. The aromatic residues on each end of the hydrophobic $(LA)_n$ core of GWALP peptides help to position the peptide termini at the respective membrane−water interfaces, at best in orientations that minimize hydrophobic mismatch between the lipid thickness and the peptide length. Deuterium-labeled (^2H) alanine residues at various positions in the core Leu−Ala sequence of each peptide then allow characterization of the behavior of the peptides in aligned bilayers by means of solid-state ^2H NMR spectroscopy. The ^2H quadrupolar splitting magnitudes $|\Delta\nu_q|$ from the alanine CD_3 (or C-D) groups serve to define a preferred tilted, dynamically averaged, orientation of the entire helix with respect to the bilayer normal in an applied magnetic field.[7,8]

On the basis of the solid-state ^2H NMR spectra (Figures S3−S5 of the Supporting Information), we observed a wide range of quadrupolar splittings for F^5 GWALP23, from 1 to 22 kHz in DLPC and 1−18 kHz in DOPC (Table 2), suggesting that the peptide helix tilts substantially in the bilayer membranes. (If the helix were not tilted, then all of the labeled alanines would give the same signal, namely, the same quadrupolar splitting, $\Delta\nu_q$.) The wide ranges of 21 and 17 kHz are consistent with those seen previously for the W5 and Y5 analogues of GWALP23, suggesting similar global helix dynamics regardless of whether the aromatic residue is capable (W5 and Y5) or not (F5) of hydrogen bonding. Indeed, the ranges of $\Delta\nu_q$ values observed when W5 is present are 23 and 14 kHz in DLPC and DOPC, respectively. The corresponding ranges when Y5 is present are 21 and 13 kHz. These large and similar ranges of $\Delta\nu_q$ in all three of the X^5GWALP23 peptides, where X is aromatic, suggest that all of these GWALP23 analogues are tilted to similar extents, and exhibit similar dynamics, in the lipid bilayer membranes.

By using an α-helical geometry and a principal order parameter S_{zz} to describe the helix motions, the sets of ^2H-alanine quadrupolar splittings can be analyzed by a method known as "geometric analysis of labeled alanines" (GALA).[10] The method finds the lowest RMSD values based on the helix tilt (τ), azimuthal rotation (ρ), and S_{zz} as variables. Notably, the resulting tilt values for F^5GWALP23 (about 7 and 21° in DOPC and DLPC, respectively) are nearly identical to those found previously[8] for the W5 and Y5 peptides (Table 3). In the shorter DLPC lipids, the average tilt of the W19 peptides with a single N-flanking aromatic residue at position five is 21°, whereas in the longer DOPC lipids, the average tilt is 6°. Comparison of these τ values for DLPC and DOPC lipids suggests that each of the X^5GWALP23 peptide responds to hydrophobic mismatch by tilting more in the thinner bilayers.

It was surprising (see Discussion) to observe that the double-Phe derivative, $F^{4,5}$GWALP23, with adjacent aromatic phenyl rings at positions 4 and 5, displays a wider range of ^2H quadrupolar splittings than does F^5GWALP23 itself. These results stand in stark contrast to the earlier comparison between $Y^{4,5}$GWALP23 and Y^5GWALP23.[8] In the shortest lipid, DLPC,

Table 2. ^2H NMR Quadrupolar Splittings ($\Delta\nu_q$, in kHz) for Labeled Alanine CD_3 Groups in F^5GWALP23, $F^{4,5}$GWALP23, and Y^4GWALP23[a]

	DLPC				DMPC		DOPC			
Ala-d_4	F^5	$F^{4,5}$	Y^4	W^5W^{18}	F^5	Y^4	F^5	$F^{4,5}$	Y^4	W^5W^{18}
7	17.8	23.7	15.8	--	--	17.6	16.2	16.2	11.8	--
9	20.4	23.5	9.2	14.9	--	6.4	2.8	0.8	1.5	6.6
11	21.9	25.7	18.8	--	--	17.9	17.6	18.6	16.4	15.4
13	13.8	19.6	9.2	9.0	--	8.5	3.4	0.8	3.2	2.3
15	18.3	23.4	18.8	25.6	--	18.4	17.6	18.6	18.4	5.6
17	1.0	1.8	1.3	21.6	--	2.7	1.0	1.9	2.2	17.2

[a]Sample orientation is $\beta = 0°$. Each value (in kHz) is the average of the magnitude observed at $\beta = 0°$ and twice the magnitude observed for a $\beta = 90°$ sample orientation. Values that are absent (--) were not recorded. The labeled alanines are identified, and the positions of the N-flanking aromatic amino acids are indicated as F^5, $F^{4,5}$, and Y^4. The C-flanking W^{19} is present in all samples except for W^5W^{18}.

dx.doi.org/10.1021/bi500439x | *Biochemistry* 2014, 53, 3637−3645

Table 3. Semistatic GALA Analysis of Transmembrane Orientations of Peptides of the GWALP23 Family[a]

	DLPC				DMPC				DOPC			
peptide	τ_0	ρ_0	S_{zz}	RMSD (kHz)	τ_0	ρ_0	S_{zz}	RMSD (kHz)	τ_0	ρ_0	S_{zz}	RMSD (kHz)
[b]W^5	21°	305°	0.71	0.7	9	311	0.88	1.0	6	323	0.87	0.6
[b]Y^5	19	295	0.78	0.7	10	300	0.84	0.7	5	311	0.84	1.0
F^5	21	310	0.58	1.1					7	330	0.85	0.6
[b]$Y^{4,5}$	5	260	0.66	1.6	3	323	0.77	0.6	3	359	0.82	1.1
$F^{4,5}$	21	317	0.67	0.6					6	332	0.92	0.9
Y^4	12	327	0.68	0.8	10	332	0.73	0.9	7	357	0.86	0.3
W^5W^{18}	19	40	0.78	1.5					12	265	0.74	1.3

[a]The N-flanking aromatic residues are indicated by the abbreviation for each peptide. C-flanking W^{19} is also present in all samples except when the aromatic residues are W^5 and W^{18}. [b]Values from ref. 17.

the range of $\Delta\nu_q$ for alanines in $F^{4,5}$GWALP23 is about 24 kHz, from 1.8 to 25.7 kHz. In DOPC, the values cover a range of about 17 kHz, from 1.9 to 18.6 kHz (Table 2). These differences suggest that $F^{4,5}$GWALP23 may be tilted to greater extent or may undergo less dynamic averaging than the single-anchored X^5GWALP23 peptides. It is striking that the results for $F^{4,5}$GWALP23 differ greatly from the previous characterization of $Y^{4,5}$GWALP23.[8] The larger quadrupolar splittings that are observed in ^{2}H NMR spectra for the F4,5 peptide are greatly reduced in the spectra for Y4,5 (Figure 3). The ranges

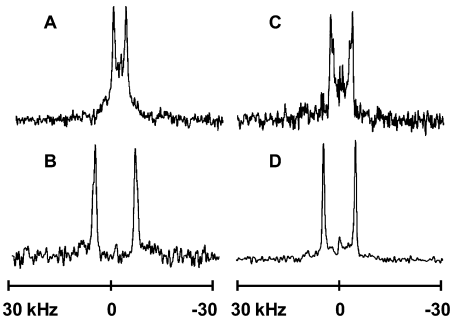

Figure 3. ^{2}H NMR spectra for labeled alanines in selected $X^{4,5}$ peptides in DLPC and DOPC: (A) $Y^{4,5}$GWALP23 in DLPC, (B) $F^{4,5}$GWALP23 in DLPC, (C) $Y^{4,5}$GWALP23 in DOPC, and (D) $F^{4,5}$GWALP23 in DOPC. In each peptide, Ala-15 is 100% deuterated and Ala-11 is 50% deuterated. β = 90° sample orientation; 50 °C.

of the quadrupolar splitting magnitudes from alanines in $Y^{4,5}$GWALP23 therefore span only 11 and 9 kHz in DLPC and DOPC, respectively (Table 2). By changing the identity of the aromatic anchors at positions 4 and 5 from Tyr to Phe (Y to F), thereby removing the hydrogen-bonding ability of the aromatic ring, the net effect is to double the kilohertz range that is spanned by the alanine quadrupolar splittings, a dramatic change! Furthermore, when comparing the change in $\Delta\nu_q$ range from DLPC to DOPC, one would expect a significant decrease due to less tilting necessary in the longer lipid. For $F^{4,5}$GWALP23, the range indeed narrows from 24 to 17 kHz from DLPC to DOPC, but for $Y^{4,5}$GWALP23, the range hardly changes. These results suggest that the Tyr (Y) anchors at positions 4 and 5 allow far less response to bilayer thickness than do the Phe (F) anchors, probably because the extent of dynamic averaging is large in both lipids when Y^4 and Y^5 are present together.

The results of tilt analysis for $F^{4,5}$GWALP23 also are strikingly different from the previous results for $Y^{4,5}$GWALP23.[8] The tilt value for $F^{4,5}$GWALP23 in DLPC (~21°) is much larger than the "apparent" tilt of the Y4,5 analogue (~5°) (Table 3). The actual tilt of $Y^{4,5}$GWALP23 in DLPC is nevertheless obscured by the extensive dynamics of this peptide.[8] Remarkably, $F^{4,5}$GWALP23 does not suffer from the high dynamics and gives quadrupolar wave fits for tilt and azimuthal rotation similar to those for F^5GWALP23 in DLPC and DOPC (Figure 4). In DLPC, the wave amplitude actually is

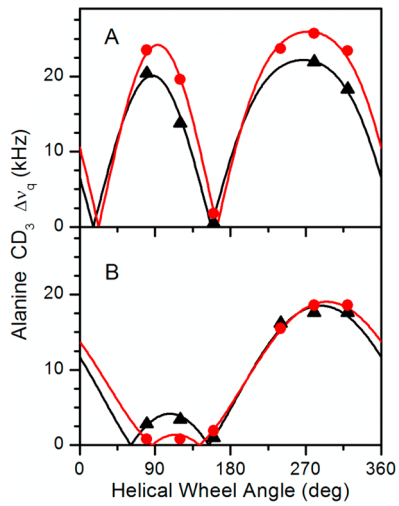

Figure 4. Quadrupolar wave plots for F^5GWALP23 (black, triangles) and $F^{4,5}$GWALP23 (red, circles) in (A) DLPC and (B) DOPC.

larger for $F^{4,5}$GWALP23 than for F^5GWALP23 (Figure 4A), suggesting somewhat lower dynamic averaging for $F^{4,5}$GWALP23, and the wave amplitudes for both $F^{4,5}$GWALP23 and F^5GWALP23 are notably very much larger than that for $Y^{4,5}$GWALP23 in DLPC.[17] In DOPC, these three peptides have rather similar small tilt angles (Figure 4B and Table 3), yet the dynamic averaging remains much larger for $Y^{4,5}$GWALP23 (see Discussion).

For the case of moving the tyrosine residue from position 5 to position 4 in the sequence, the helix tilt and dynamics remain unchanged, yet a phase change is seen in the quadrupolar wave plot (Figure 5), indicating a change in the helix azimuthal rotation (ρ_o) or direction of the tilt. Semistatic GALA analysis of Y^4GWALP23 indicates that the rotation of the peptide changes by about 31° in DLPC and 46° in DOPC (Table 3) when Y5 is moved radially by 100° to position 4. A top view or helical wheel illustrates these differences in the direction of tilt for Y^4GWALP23 and Y^5GWALP23 (Figure 5B). Importantly, the extensive dynamics observed for double-Tyr derivative $Y^{4,5}$GWALP23 are not caused by either Y4 or Y5 alone, but rather by the presence of the two tyrosines together.

dx.doi.org/10.1021/bi500439x | Biochemistry 2014, 53, 3637−3645

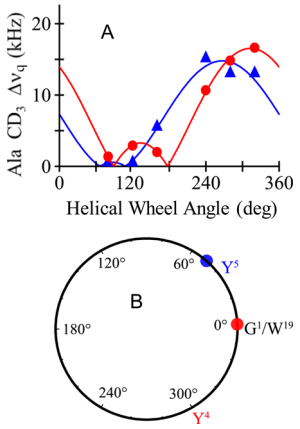

Figure 5. (A) Quadrupolar wave plots for Y^4GWALP23 (red, circles) and Y^5GWALP23 (blue, triangles) in DOPC. (B) Helical wheel diagram to illustrate the relative azimuthal rotation ρ for Y^4GWALP23 (red circle) and Y^5GWALP23 (blue circle) in DOPC, offset by ~50°. The labels Y^4 and Y^5 represent the respective radial locations of the tyrosines, which differ by 100° on the helical wheel.

Because of the change in azimuthal rotation that accompanies the moving of Y5 to Y4, we decided to investigate the consequence of moving W19 to position 18 in GWALP23. The results (Figure 6) indicate a larger rotational shift of almost

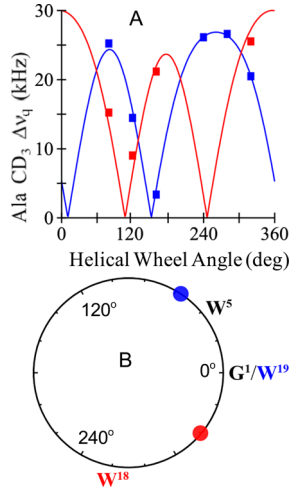

Figure 6. (A) Quadrupolar wave plots for W^{18}GWALP23 (red) and GWALP23 itself (blue) in DLPC. (B) Helical wheel diagram to illustrate the relative azimuthal rotation ρ for W^{18}GWALP23 (red circle) in relation to (W^{19})GWALP23 (blue circle) in DLPC, offset by ~100°. The labels W^{18} and W^{19} represent the respective radial locations of the tryptophans, which differ by 100° on the helical wheel.

100° for the peptide helix in DLPC when W19 in GWALP23 is moved by 100° to W18. This large shift suggests a dominant role for W19 in determining the azimuthal rotation preference of GWALP23 in lipid bilayer membranes. Yet, a similar comparison between GWALP23 and W^{18}GWALP23 in DOPC brings a surprise (Table 3). Namely, the preferred azimuthal rotation of the W^{18}GWALP23 helix seems to depend upon the lipid environment. Within the realm of transmembrane peptides that exhibit low dynamic averaging, this result for W^{18}GWALP23 stands in contrast to the essentially constant rotational preferences of other GWALP23 family peptides in bilayers of differing thickness.[12] Namely, for the transmembrane helices of GWALP23, $R^{2,22}$GWALP23, and $K^{2,22}$GWALP23,[12] as well as R^{14}GWALP23,[14,18] Y^5GWALP23,[17] Y^{19}GWALP23,[26] Y^4GWALP23, F^5GWALP23, and $F^{4,5}$GWALP23 (this work), the most probable azimuthal rotation ρ_o about the helix axis does not vary appreciably when each particular helix is moved from DLPC to DMPC or DOPC. For cases of excess dynamics, namely, $W^{2,22}$GWALP23[12] and $Y^{4,5}$GWALP23,[17] which also incorporate extra aromatic residues, σ_ρ is large and ρ_o is not well defined from lipid to lipid. In this respect, W^{18}GWALP23 stands alone with low dynamic averaging and yet has a value of ρ_o that changes by about 135° from DLPC to DOPC (Table 3). Even if one considers a Gaussian analysis (see Discussion), the value of ρ_o still varies widely from DLPC to DOPC. We therefore sought to consider possible reasons for this lipid-dependent variation in helix azimuthal rotation.

Recently,[23] a method was presented for correlating helix rotational preference with flanking residue positions on a tilted transmembrane helix. We have applied this method to W^{18}GWALP23 (Figure 7) as well as to the parent GWALP23

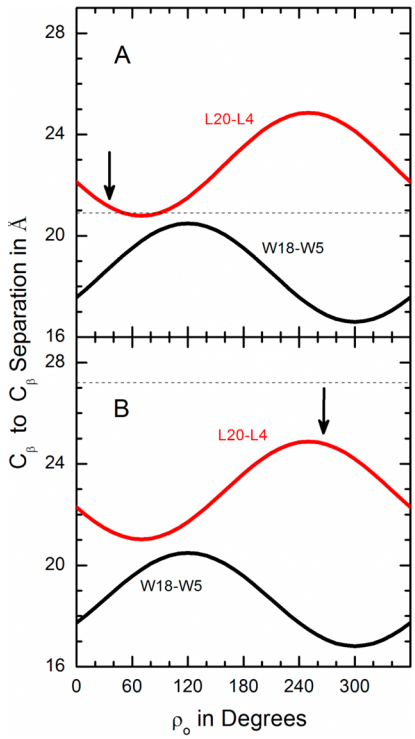

Figure 7. Aromatic (W18–W5) and hydrophobic (L20–L4) residue C_β separation distances in angstroms along the bilayer normal as functions of rotation of W^{18}GWALP23 about its tilted helix axis (A) when τ_o = 18° in DLPC or (B) when τ_o = 17° in DOPC. The preferred ρ_o values are shown by the arrows. The respective bilayer thicknesses are indicated by the dashed segments.

helix (Figure 8). These peptides are sequence isomers that differ only with respect a substitution of $W^{18}L^{19}$ in place of $L^{18}W^{19}$; yet, their rotational preferences are remarkably different. A flanking residue analysis suggests that the rotation of W^{18}GWALP23 is governed not by the W18-to-W5 distance (along the bilayer normal) but perhaps by the L20-to-L4 distance (Figure 7). Indeed, the tilted W^{18}GWALP23 helix rotates about its axis to give approximately the minimum L20-to-L4 distance in DLPC (Figure 7A) and approximately the

dx.doi.org/10.1021/bi500439x | Biochemistry 2014, 53, 3637−3645

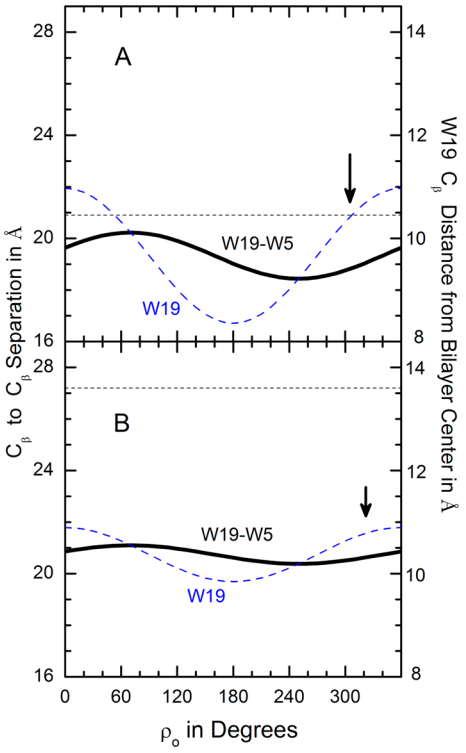

Figure 8. Aromatic residue C_β separation distance along the bilayer normal and W19 C_β distance from bilayer center as functions of rotation of GWALP23 about its tilted helix axis (A) when $\tau_o = 23°$ in DLPC or (B) when $\tau_o = 9°$ in DOPC. The preferred ρ_o values are shown by the arrows. The respective bilayer thicknesses are indicated by the dashed segments.

maximum L20-to-L4 distance in DOPC (Figure 7B). Notably, the tilt angle for W^{18}GWALP23 appears to be essentially the same in DOPC as in DLPC (Table 3, Figure 7), with the main adaption seeming to involve the helix rotation. We will revisit these issues using a modified Gaussian analysis (see Discussion).

However, the rotation of GWALP23 (Figure 8) seems not to correlate with either the W19-to-W5 distance or the L20-to-L4 distance. Indeed, we surmise that W19 itself may play a special role. Being near the C-terminal, the indole side chain of W19 must adopt non-standard torsion angles[27,28] in order to aim its NH bond toward the aqueous solution. Furthermore, the helix properties are more sensitive to substitution of W19 by Tyr than to substitution of W5 by Tyr,[26] again suggesting a special role for the W19 indole. Within this context, the tilted GWALP23 helix in DLPC is rotated so as to provide an (perhaps fortuitous) exact match between the W19 C_β distance from the bilayer center and half of the DLPC bilayer's hydrophobic thickness (Figure 8A). In the thicker DOPC, the GWALP23 helix is less tilted such that the W19 C_β position, with respect to the bilayer center, varies less steeply with rotation (Figure 8B). There is a detectable, yet minor, change in ρ_o, so as to move the W19 side chain outward, but only slightly, with the main adaption being the smaller helix tilt in the thicker lipid bilayer. In contrast, W^{18}GWALP23 adapts to the changing lipid environment more by changing its helix rotation than by changing its tilt (Figure 7).

DISCUSSION

Recent reports have compared the influence of Tyr versus Trp in the N-flanking position 5[17] and the C-flanking position 19 [26] in membrane-spanning GWALP23 peptides. The main findings were that either Tyr or Trp at each location will support a similar tilted transmembrane helix orientation, with only about a 10 relative azimuthal rotation about the helix axis when Tyr is substituted for Trp. Furthermore, the extent of dynamic averaging of solid-state NMR observables remains low as long as only one interfacial aromatic residue is present at each end of the membrane-spanning GWALP23 helix (with no extra aromatic residues potentially competing for lipid headgroup interactions).

In the present work, we compare the results for Trp/Tyr with the consequences of Phe substitutions at positions 4 and 5 in GWALP23. Additionally, we examine the consequences of moving a single aromatic side chain, either Y5 or W19, 100° around the helix axis by interchanging either Y5 and L4 or W19 and L18. Key findings are (a) an unexpectedly low extent of dynamic averaging for $F^{4,5}$GWALP23 and (b) a preference of azimuthal rotation of W^{18}GWALP23 that depends upon the identity (thickness) of the host lipid bilayer membrane. We will discuss first the results with the tyrosine-to-phenylalanine substitutions. Because of the differences in dynamics, we will also present the outcomes for a modified Gaussian treatment of the helix rotational dynamic averaging. Then, we will discuss the changes in rotational preference when aromatic and leucine residue locations are switched on the N-flanking side or the C-flanking side of the core helix.

Changes Involving Y5 → F5 or Y4,Y5 → F4,F5. A significant question concerns the hydrogen-bonding property of the OH group on the Y5 ring, which could interact favorably, albeit transiently (under conditions of dynamic hydrogen-bond exchange), with lipid heads groups and interfacial water molecules. The potential for hydrogen bonding is nevertheless absent when the F5 phenyl ring is substituted for Y5. With F^5GWALP23, we find that hydrogen bonding by the N-flanking aromatic ring is not necessarily needed to define a preferred, stable transmembrane orientation, with limited dynamic averaging, for the core $(LA)_6L$ transmembrane helix. In this context, the indole ring of W19 seems to have special importance for defining the orientation and low dynamics (see below) and should not be overlooked or underestimated. Notably, F^5GWALP23 exhibits a similar transmembrane orientation as that of Y^5GWALP23 and W^5GWALP23 (Figure 4 and Table 3), with low dynamic averaging. Furthermore, F^5GWALP23, as well as its Y5 and W5 cousins, adapts to changes in the lipid bilayer thickness mainly by changing its tilt (Figure 4 and Table 3), with little change of the helix azimuthal rotation. The slightly smaller amplitude of the quadrupolar wave for F^5GWALP23 in DLPC (Figure 4) nevertheless suggests increased dynamic averaging, which indeed is borne out by the lower estimate of 0.58 for S_{zz} for F^5GWALP23 in DLPC (Table 3). This order parameter is notably low compared to those observed for gramicidin A[29] and Y^5GWALP23 or GWALP23 itself (Table 3). Moreover, we note the uniformly lower estimates for S_{zz} from the semistatic GALA analysis of each peptide helix in DLPC compared to DOPC (Table 3).

The change from $Y^{4,5}$GWALP23 to $F^{4,5}$GWALP23 brings big changes to the properties of the transmembrane helix, mainly to reduce the very extensive dynamic averaging that occurs when

dx.doi.org/10.1021/bi500439x | Biochemistry 2014, 53, 3637−3645

Y4 and Y5 are present together. It has been noted that $Y^{4,5}$GWALP23 exhibits dramatically more dynamic averaging than is the case when only one tyrosine is present in Y^{5}GWALP23.[17] What happens when the hydrogen-bonding ability is removed from the Y4 and Y5 aromatic rings? Remarkably, the dynamic averaging is seen to diminish when F4 and F5 are present (compare Figure 4 to Figure 6B in ref 17). We surmise that the phenyl rings of F4 and F5 are favorably placed if they are just "in the neighborhood" of the interfacial region, without need of any specific interactions with the lipid head groups. Phenol rings Y4 and Y5, on the other hand, may compete, perhaps alternately, for direct hydrogen-bonding interactions with lipid head groups. Such competition, if not able to optimize simultaneously a Y4 interaction and a Y5 interaction, could lead to increased helix rotational dynamics of the type suggested previously.[11,13] Importantly, neither Y4 nor Y5 alone causes the extensive dynamic averaging (see below); rather, it is the pair of tyrosines together that leads to the high level of dynamics, as has been noted also for pairs of tryptophans.[12]

Modified Gaussian Treatment of the Dynamics. We sought to compare a semistatic treatment with a modified Gaussian treatment of the dynamic properties of each of the transmembrane peptides. The semistatic GALA treatment[7,8] employs three adjustable parameters: tilt, τ_o, and azimuthal rotation, ρ_o, to describe helix orientation, together with a principal order parameter, S_{zz}, to provide a highly abbreviated estimate of overall dynamics. A Gaussian treatment offers advantages of describing estimates for helix "wobble" σ_τ and rotational "slippage" σ_ρ, but it does so at the expense of requiring four adjustable parameters instead of three.[13] As an alternative, a modified Gaussian treatment has been suggested,[16] in which σ_τ is held constant and dynamic differences are embodied in an adjustable σ_ρ. We have employed this modified procedure[16] but differing in that we set σ_τ to a small finite value instead of to zero while maintaining S_{zz} of 0.88 as an estimate of internal motion of the peptide.[14]

Notably, the results of such a modified Gaussian analysis (Table 4) agree substantially with the conclusions from a semistatic GALA analysis (Table 3). Both methods indicate that each peptide (except possibly W^{18}GWALP23; see below) adapts from DOPC to DLPC by increasing its tilt. The methods in all cases give the same preferred values of ρ_o in each lipid and are in agreement concerning the small variations when the identity of aromatic residue 5 is changed. Additionally, the same trends for in ρ_o are seen with either method when a peptide helix is moved from DOPC to DLPC. Generally, the change of lipid involves only a small $\Delta\rho_o$, excepting the case of W^{18}GWALP23 (see below) and the highly dynamic $Y^{4,5}$GWALP23, noted previously.[17]

The respective outcomes for fitting the dynamics also are similar. The semistatic analysis (Table 3) leads to estimates for S_{zz} that are higher in DOPC than in DLPC, seemingly because the relatively smaller tilt angles in DOPC do not demand a downgrade of S_{zz} during the fitting process. For the modified Gaussian analysis, we set σ_τ to 15° in DLPC (where τ_o is larger) and to 9° in DOPC (where τ_o is smaller). (When presented with a binary choice of either 9 or 15°, the analytical software selected 15° for each peptide in DLPC but 9° for each peptide in DOPC; the values subsequently were fixed.) With these constraints, the resulting fitted values for σ_ρ are similar between DLPC and DOPC (Table 4), with somewhat larger values of σ_ρ emerging for the fits in DOPC (perhaps reflecting the somewhat smaller choice for σ_τ). For the highly dynamic $Y^{4,5}$GWALP23, σ_ρ is seen to be very large in both DLPC and DOPC, thereby confirming earlier conclusions based on semistatic analysis.[17] With a caveat that the helix behavior should be examined in more than one lipid, similar conclusions about the extent of dynamic averaging (whether limited, moderate, or high) for each transmembrane helix emerge from the semistatic GALA and modified Gaussian analyses. It is useful and productive to apply and compare both methods.

Table 4. Modified Gaussian Analysis of Orientations and Dynamics for Peptides of the GWALP23 Family[a,b]

	DLPC				DOPC			
peptide	τ_0	ρ_0	$\sigma\rho$	RMSD (kHz)	τ_0	ρ_0	$\sigma\rho$	RMSD (kHz)
W^5	23	304	33	0.7	9	321	48	0.7
Y^5	23	295	32	0.0	6	313	34	1.0
F^5	17	314	21	1.7[c]	9	329	40	0.6
$Y^{4,5}$	14	259	>90[d]	1.7	6	344	72	0.9[e]
$F^{4,5}$	18	314	0[f]	0.7	10	329	54	1.6
Y^4	11	328	22	0.9	11	353	56	0.4
W^5W^{18}	18	35	8[f]	1.4	17	264	50	1.2

[a]The N-flanking aromatic residues are indicated by the abbreviation for each peptide. C-flanking W^{19} is also present in all samples except when the aromatic residues are W^5 and W^{18}. [b]Analysis followed Strandberg et al.,[16] but $\sigma\tau$ was assigned a finite value instead of 0° (see Methods). Except as noted, $\sigma\tau$ was set to 15° in DLPC or 9° in DOPC. [c]The value of $\sigma\tau$ was 20° because no satisfactory solution was found when $\sigma\tau$ = 15°. [d]The value of $\sigma\rho$ remains > 90° even if $\sigma\tau$ is set to 20°. [e]The value of $\sigma\tau$ was 13° because no satisfactory solution was found when $\sigma\tau$ = 9°. [f]The value of $\sigma\rho$ is perhaps artificially low because of the choice of $\sigma\tau$. Because of the limited data set, further solutions were not explored.

Changes in Rotational Preference when Y5 Is Moved or W18 Is Moved. We observed sizable changes in the preference for helix azimuthal rotation when a key aromatic ring, the side chain of either residue 5 or residue 19, has been moved by 100° around the helix axis (Tables 3 and 4). In this regard, the Trp residue, W19, seems once again to have a special importance, as the changes to the rotational preference are larger and lipid-dependent when this tryptophan is moved.

When Y4 is moved to Y5, the preferred ρ_o changes by about 30−35° in DLPC and by about 40−45° in DOPC. Conspicuously, the deduced values of $\Delta\rho_o$ are similar between the semistatic and modified Gaussian methods of analysis (Tables 3 and 4). The rotational change furthermore is slightly less than half of the 100° radial shift that accompanies the move of Tyr from position 5 to position 4. The results suggest that a compromise may be imposed by the interplay of W19 (fixed) and either Y4 or Y5 (variable), with the influence of W19 on the rotational preference nevertheless dominating to a small extent over that of Y4 or Y5 (because $\Delta\rho_o$ < 50° in both lipids). We recall also that the identity of residue 5 exerts a smaller influence on the azimuthal rotation.[17] Interestingly, ρ_o decreases ∼10° when W5 is changed to Y5, but it increases ∼10° when W5 is changed to F5; the molecular reasons that may underlie these small but opposite values of $\Delta\rho_o$ are elusive at this time.

The movement of W19 to position 18 has major influence on the helix azimuthal rotation. Interestingly, an interchange of W19 and L18 leads to a change in ρ_o of +90° in DLPC but −60° in DOPC in spite of the fact that σ_ρ remains low in DLPC and moderate in DOPC (Tables 3 and 4). These results

dx.doi.org/10.1021/bi500439x | Biochemistry 2014, 53, 3637−3645

once again highlight the major importance of W19, or more generally of the C-flanking aromatic residue, for the helix azimuthal rotation. Moreover, the semistatic and modified Gaussian methods agree on not only the absolute magnitudes but also the extent of change in both lipids (Tables 3 and 4). Why does the preferred rotation of W^{18}GWALP23, but not of the other peptides that experience low dynamic averaging, depend upon the host lipid bilayer? While the possible answers to this question remain incomplete at this time, some clues may emerge from consideration of Figures 7 and 8. With W18 and W5 separated by 140° on the helical wheel (Figures 1 and 6), the transmembrane helix azimuthal rotation seems not to correlate with the W5-to-W18 separation distance along the bilayer normal (Figure 7) but rather with the L4-to-L20 distance, which could better describe the longitudinal hydrophobic length of the helix. Indeed, W^{18}GWALP23 seemingly rotates so as to minimize the L4-to-L20 transmembrane distance in DLPC and to maximize the L4-to-L20 transmembrane distance in DOPC (Figure 7). While more examples would be needed to establish a causal relationship instead of a mere correlation, this principle could help to explain the lipid-dependent helix rotation for the special case of the W^{18}GWALP23 helix.

The particular importance of W19 for the transmembrane orientation of GWALP23 is evident in Figure 8. Notably, in GWALP23, the two Trp residues are on the same side of a helical wheel, with a radial displacement of only 40° (Figures 1 and 5). Rather than any dependence on the W5-to-W19 longitudinal separation, GWALP23 rotates in DLPC so that the distance from C_β of W19 to the bilayer center matches the hydrophobic thickness of a DLPC monolayer (Figure 8A). From DLPC to DOPC, the main adjustment is that GWALP23 is less tilted in DOPC. The rather minimal rotational adjustment serves to move W19 slightly farther away from the DOPC bilayer center (Figure 8B).

CONCLUDING REMARKS

For the model membrane-spanning helix of acetyl-GGALW-$(LA)_6$LWLAGA-amide (GWALP23), a well-defined transmembrane orientation with only limited dynamic averaging, other than long-axis precession about the bilayer normal,[9] is retained following the single aromatic residue substitution of F5 or Y5 in place of W5. By contrast, all known model transmembrane peptide helices having more than two interfacial Trp or Tyr residues characterized to date exhibit extensive dynamic averaging of the solid-state NMR observables. Remarkably, nevertheless, the peptide $F^{4,5}GW^{19}$ALP23 fits into the category of low dynamics and not high dynamics, perhaps because of the absence of hydrogen-bonding ability of the phenyl rings. Y5 confers similar properties as W5. When the single Y5 is moved to Y4, within the context where W19 is held constant to flank the other end of the core helix, there ensues a change of about 40° in the preferred helix azimuthal rotation regardless of whether the host lipid membrane is DLPC or DOPC. By contrast, when the single W19 is moved to W18, within the context where W5 is held constant to flank the other end of the core helix, the preferred helix azimuthal rotation is seen to vary greatly, by ∼130°, between DLPC and DOPC. The results suggest that a dynamic interplay between lipid membrane thickness and protein helix rotation may regulate aspects of biological function.

ASSOCIATED CONTENT

Supporting Information

^{2}H NMR, ^{31}P NMR, and mass spectra. This material is available free of charge via the Internet at http://pubs.acs.org.

AUTHOR INFORMATION

Corresponding Author

*Tel.: (479) 575-4976; Fax: (479) 575-4049; E-mail: rk2@uark.edu.

Funding

This work was supported in part by NSF MCB grant 1327611 and by the Arkansas Biosciences Institute. The peptide, NMR, and mass spectrometry facilities are supported by NIH grants GM103429 and GM103450.

Notes

The authors declare no competing financial interest.

ACKNOWLEDGMENTS

We thank Vitaly Vostrikov for software for semistatic GALA and modified Gaussian methods for analysis of helix orientations and dynamics.

ABBREVIATIONS USED

CD, circular dichroism; DLPC, 1,2-dilauroylphosphatidylcholine; DMPC, 1,2-dimyristoylphosphatidylcholine; DOPC, 1,2-dioleoylphosphatidylcholine; Fmoc, fluorenylmethoxycarbonyl; GALA, geometric analysis of labeled alanines; GWALP23, acetyl-GGALW$(LA)_6$LWLAGA-[ethanol]amide; MtBE, methyl-*t*-butyl ether; RMSD, root mean squared deviation; TFA, trifluoroacetic acid; WWALP23, acetyl-GWALW-$(LA)_6$LWLAWA-[ethanol]amide

REFERENCES

(1) O'Connell, A. M., Koeppe, R. E., II, and Andersen, O. S. (1990) Kinetics of gramicidin channel formation in lipid bilayers: transmembrane monomer association. *Science 250*, 1256−1259.

(2) Schiffer, M., Chang, C. H., and Stevens, F. J. (1992) The functions of tryptophan residues in membrane proteins. *Protein Eng. 5*, 213−214.

(3) Landolt-Marticorena, C., Williams, K. A., Deber, C. M., and Reithmeier, R. A. (1993) Non-random distribution of amino acids in the transmembrane segments of human type I single span membrane proteins. *J. Mol. Biol. 229*, 602−608.

(4) Killian, J. A., Salemink, I., de Planque, M. R., Lindblom, G., Koeppe, R. E., II, and Greathouse, D. V. (1996) Induction of nonbilayer structures in diacylphosphatidylcholine model membranes by transmembrane alpha-helical peptides: importance of hydrophobic mismatch and proposed role of tryptophans. *Biochemistry 35*, 1037−1045.

(5) de Planque, M. R., Kruijtzer, J. A., Liskamp, R. M., Marsh, D., Greathouse, D. V., Koeppe, R. E., II, de Kruijff, B., and Killian, J. A. (1999) Different membrane anchoring positions of tryptophan and lysine in synthetic transmembrane alpha-helical peptides. *J. Biol. Chem. 274*, 20839−20846.

(6) de Planque, M. R., Boots, J. W., Rijkers, D. T., Liskamp, R. M., Greathouse, D. V., and Killian, J. A. (2002) The effects of hydrophobic mismatch between phosphatidylcholine bilayers and transmembrane alpha-helical peptides depend on the nature of interfacially exposed aromatic and charged residues. *Biochemistry 41*, 8396−8404.

(7) van der Wel, P. C., Strandberg, E., Killian, J. A., and Koeppe, R. E., II. (2002) Geometry and intrinsic tilt of a tryptophan-anchored transmembrane alpha-helix determined by ^{2}H NMR. *Biophys. J. 83*, 1479−1488.

(8) Strandberg, E., Ozdirekcan, S., Rijkers, D. T., van der Wel, P. C., Koeppe, R. E., II, Liskamp, R. M., and Killian, J. A. (2004) Tilt angles

of transmembrane model peptides in oriented and non-oriented lipid bilayers as determined by ^{2}H solid-state NMR. *Biophys. J. 86*, 3709−3721.
(9) Lee, J., and Im, W. (2008) Transmembrane helix tilting: Insights from calculating the potential of mean force. *Phys. Rev. Lett. 100*, 018103.
(10) Özdirekcan, S., Etchebest, C., Killian, J. A., and Fuchs, P. F. J. (2007) On the orientation of a designed transmembrane peptide: toward the right tilt angle? *J. Am. Chem. Soc. 129*, 15174−15181.
(11) Esteban-Martín, S., and Salgado, J. (2007) The dynamic orientation of membrane-bound peptides: bridging simulations and experiments. *Biophys. J. 93*, 4278−4288.
(12) Vostrikov, V. V., Daily, A. E., Greathouse, D. V., and Koeppe, R. E., II. (2010) Charged or aromatic anchor residue dependence of transmembrane peptide tilt. *J. Biol. Chem. 285*, 31723−31730.
(13) Strandberg, E., Esteban-Martin, S., Salgado, J., and Ulrich, A. S. (2009) Orientation and dynamics of peptides in membranes calculated from ^{2}H-NMR data. *Biophys. J. 96*, 3223−3232.
(14) Vostrikov, V. V., Grant, C. V., Opella, S. J., and Koeppe, R. E., II. (2011) On the combined analysis of ^{2}H and ^{15}N/^{1}H solid-state NMR data for determination of transmembrane peptide orientation and dynamics. *Biophys. J. 101*, 2939−2947.
(15) Vostrikov, V. V., Grant, C. V., Daily, A. E., Opella, S. J., and Koeppe, R. E., II. (2008) Comparison of "polarization inversion with spin exchange at magic angle" and "geometric analysis of labeled alanines" methods for transmembrane helix alignment. *J. Am. Chem. Soc. 130*, 12584−12585.
(16) Strandberg, E., Esteban-Martin, S., Ulrich, A. S., and Salgado, J. (2012) Hydrophobic mismatch of mobile transmembrane helices: Merging theory and experiments. *Biochim. Biophys. Acta 1818*, 1242−1249.
(17) Gleason, N. J., Vostrikov, V. V., Greathouse, D. V., Grant, C. V., Opella, S. J., and Koeppe, R. E., II (2012) Tyrosine replacing tryptophan as an anchor in GWALP peptides. *Biochemistry 51*, 2044−2053.
(18) Vostrikov, V. V., Hall, B. A., Greathouse, D. V., Koeppe, R. E., II, and Sansom, M. S. P. (2010) Changes in transmembrane helix alignment by arginine residues revealed by solid-state NMR experiments and coarse-grained MD simulations. *J. Am. Chem. Soc. 132*, 5803−5811.
(19) Vostrikov, V. V., Hall, B. A., Sansom, M. S. P., and Koeppe, R. E., II. (2012) Accommodation of a central arginine in a transmembrane peptide by changing the placement of anchor residues. *J. Phys. Chem. B 116*, 12980−12990.
(20) Gleason, N. J., Vostrikov, V. V., Greathouse, D. V., and Koeppe, R. E., II. (2013) Buried lysine, but not arginine, titrates and alters transmembrane helix tilt. *Proc. Natl. Acad. Sci. U.S.A. 110*, 1692−1695.
(21) Siegel, D. P., Cherezov, V., Greathouse, D. V., Koeppe, R. E., II, Killian, J. A., and Caffrey, M. (2006) Transmembrane peptides stabilize inverted cubic phases in a biphasic length-dependent manner: Implications for protein-induced membrane fusion. *Biophys. J. 90*, 200−211.
(22) Davis, J. H., Jeffrey, K. R., Bloom, M., Valic, M. I., and Higgs, T. P. (1976) Quadrupolar echo deuteron magnetic resonance spectroscopy in ordered hydrocarbon chains. *Chem. Phys. Lett. 42*, 390−394.
(23) Sánchez-Munoz, O. L., Strandberg, E., Esteban-Martín, E., Grage, S. L., Ulrich, A. S., and Salgado, J. (2013) Canonical azimuthal rotations and flanking residues constrain the orientation of transmembrane helices. *Biophys. J. 104*, 1508−1516.
(24) Kučerka, N., Liu, Y., Chu, N., Petrache, H. I., Tristram-Nagle, S., and Nagle, J. F. (2005) Structure of fully hydrated fluid phase DMPC and DLPC lipid bilayers using X-ray scattering from oriented multilamellar arrays and from unilamellar vesicles. *Biophys. J. 88*, 2626−2637.
(25) Liu, Y., and Nagle, J. F. (2004) Diffuse scattering provides material parameters and electron density profiles of biomembranes. *Phys. Rev. E 69*, 040901 (R).
(26) Gleason, N. J., Greathouse, D. V., Grant, C. V., Opella, S. J., and Koeppe, R. E., II. (2013) Single tryptophan and tyrosine comparisons in the N-terminal and C-terminal interface regions of transmembrane GWALP peptides. *J. Phys. Chem. B 117*, 13786−13794.
(27) van der Wel, P. C., Reed, N. D., Greathouse, D. V., and Koeppe, R. E., II. (2007) Orientation and motion of tryptophan interfacial anchors in membrane-spanning peptides. *Biochemistry 46*, 7514−7524.
(28) Vostrikov, V. V., and Koeppe, R. E., II. (2011) Response of GWALP transmembrane peptides to changes in the tryptophan anchor positions. *Biochemistry 50*, 7522−7535.
(29) Separovic, F., Pax, R., and Cornell, B. (1993) NMR order parameter analysis of a peptide plane aligned in a lyotropic liquid crystal. *Mol. Phys. 78*, 357−369.
(30) DeLano, W. L. (2002) *The PyMOL Molecular Graphics System*, DeLano Scientific, San Carlos, CA.